Installation of creepmeters on the western Dinaric Faults

Vgradnja creepmetrov na zahodne Dinarske prelome

Uroš Novak[1], Roger Bilham[2]

Abstract

Hall effect creepmeters represent a cost-effective and fairly easy to maintain extensometers that record shallow slip or creep on active faults and are primarily positioned on the world`s more seismically active faults with fast deformation rates. As of the year 2022 a project of creep monitoring of the western Dinaric Faults in Slovenia (Idrija, Raša, Predjama) started, with the installment of 3 creepmeters on Idrija and Raša Faults. The aims of the project are to investigate wherever the Dinaric Faults aseismically creep or if the fault segments are locked in the interseismic period. Such insights into the mechanics of Dinaric Faults could potentially improve insights of earthquake hazard in the Dinarides.

Povzetek

Creepmetri, ki temeljijo na Hall-ovem učinku, predstavljajo ekstenzometre, ki so stroškovno učinkoviti in precej enostavni za vzdrževanje. Inštrumenti so namenjeni beleženju plitvih zdrsov ali lezenja, aktivnih prelomov. Povečini so nameščeni na svetovno seizmično bolj aktivnih prelomih z hitrimi stopnjami deformacij. Leta 2022 se je začel projekt spremljanja lezenja zahodnih dinarskih prelomov v Sloveniji (Idrija, Raša, Predjama), s postavitvijo treh creepmetrov na prelomih Idrija in Raša. Cilj tega projekta je raziskati ali zahodni dinarski prelomi aseizmično lezejo oziroma ali so segmenti prelomov zaklenjeni v medseizmičnem obdobju. Takšen vpogled v mehaniko dinarskih prelomov bi lahko potencialno izboljšal razumevanje potresne nevarnosti v Dinarskem gorstvu.

Ključne besede: creepmeter, lezenje, premiki prelomov, aktivna tektonika, Dinarski prelomni sistem, Slovenija.

Keywords: creepmeter, creep, fault displacements, active tectonics, Dinaric Fault system, Slovenia.

Fault shallow creep

Laboratory investigations of rock friction indicate that rocks typically display velocity-strengthening behavior under low temperature and normal stress conditions (Blanpied et al., 1991 Lindsey et al., 2014, passim). This suggests that the near-surface regions of active faults are prone to experiencing stable sliding or creep during the interseismic period (Lindsey et al., 2014). This hypothesis is supported from numerical simulations of faults controlled by rate-state friction. Even if friction is not inherently velocity-strengthening, these models demonstrate stable sliding at low normal stress (Kaneko et al., 2013, Lindsey et al., 2014).

[1] ZRC SAZU Inštitut za raziskovanje krasa, Titov trg 2, Postojna; Univerza v Novi Gorici, Vipavska 13, Nova Gorica

[2] Cooperative Institute for Research in Environmental Sciences at the University of Colorado Boulder, 216 UCB, University of Colorado Boulder campus, Boulder, CO 80309, ZDA

Observations of shallow interseismic creep align with the models and are documented on several seismically active faults (Lindsey et al., 2014). Examples include segments of the San Andreas Fault (the Rodgers Creek Fault, Hayward Fault, Imperial Fault and Superstition Hills Fault) in California, as well as a segment of the North Anatolian Fault (Lindsey et al., 2014) and Eastern Anatolian Fault in Turkey (Bilham et al., 2023). Additionally, some faults exhibit continuous creep across the entire seismogenic layer, such as the northern section of the San Andreas Fault (SAF) near Parkfield (Tong et al., 2013) and a portion of the Haiyuan Fault in China (Jolivet et al., 2013).

However, it's worth noting that such behaviour is not ubiquitous, given that numerous other faults don't experience interseismic creep at the surface (Lindsey et al., 2014). For instance, the Southern San Andreas Fault (SAF; Tong, 2013), the majority of the North Anatolian Fault, and the Altyn Tagh Fault in Tibet exhibit little to no interseismic creep. Because the accumulation of potential seismic moment may be significantly reduced by the occurrence of shallow creep, the latter plays an important role in our understanding of fault mechanics and earthquake hazard (Lindsey et al., 2014, Bilham et al., 2023).

Creepmeter instrumentation

Each creepmeter installed is an extensometer that uses a 6 mm diameter carbon-fiber rod as a length standard, buried obliquely across the surface trace of an active fault (Fig. 1, 2). The 10–20 m long carbon rod slides within a 2 cm diameter PVC conduit buried 30–50 cm deep across the fault, and one end is fastened rigidly to a buried anodized aluminum quadropod (passive end).

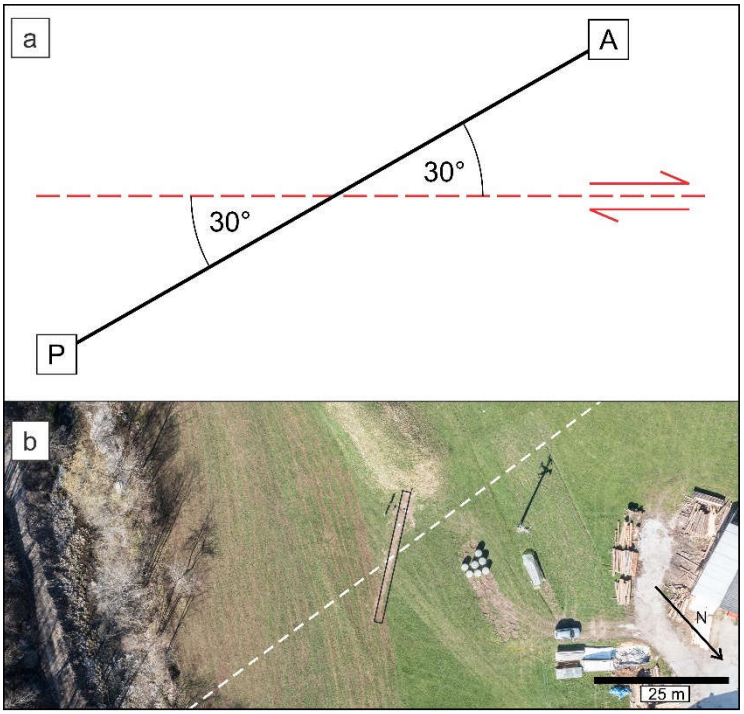

Figure 1: Creepmeter deployment scheme across a fault. a) Idealized diagram of the deployment. b) The rig deployment on the Idrija Fault (photograph author: Žan Kafol).

The free end (active end) of the rod is held in 1 N tension by a 0.1 mm diameter, multistrand, stainless-steel wire wrapped once around the 3.175 mm diameter shaft of a 360°

continuous rotation, Hall effect sensor with a linearity of <0:3%. The effective circumference of the shaft including a correction for the thickness of the 19 strand, nylon coated, stainless-steel wire is approximately 10 mm. The free end of the wire is fed by a constant tension spring motor with 1–3 m of range.

Slip on the fault pulls the rod through the conduit, which results in rotation of the shaft of the sensor (Fig. 2). The resulting 0–5 V 12-bit output is recorded by a 16-bit data logger yielding a fault-slip resolution of 2 μm (Bilham and Castillo, 2020). Monotonic slip exceeding 10 mm resets the 0–5 V signal to zero, and hence the creepmeter has a wide cumulative measurement range, and, unless an earthquake with >1 m slip occurs, no adjustments are needed during its lifetime (Bilham and Castillo, 2020).

Extensometers discussed here were installed by two or more people in 3 days using just a shovel and a pick, one site with an excavator. Initial settlement is rapid, and stable readings are usually available within a day of installation. Despite their shallow burial (20–50 cm), temperature effects are small (<2 μm=°C=m) due to the similar expansion coefficients of carbon-fiber composites and surface soils.

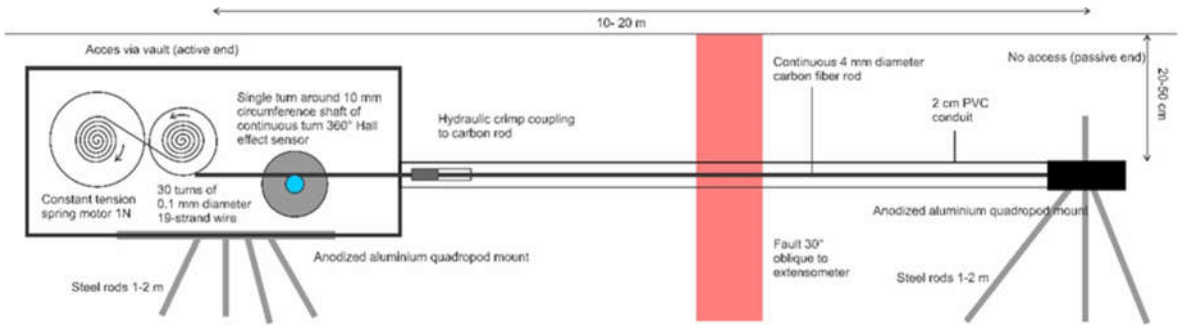

Figure 2: Schematic view of the extensometer.

Where telemetry is inadvisable due to potential vandalism, the creepmeter can be totally buried and will operate for a year from disposable alkaline batteries. To conserve power, the autonomous data logger switches the power to the sensor for 0.1 s once per minute. An obliquely installed extensometer is an imperfect measure of fault creep because it assumes that the two sides of the fault act as rigid blocks separated by an infinitely thin fault plane. If the length standard remains straight, fault creep = extension/cos(obliquity). In the extensometers described here, this geometry is approximated by a fault shear zone that after sufficient fault slip has occurred will impose an arctan curve on the initially straight rod. In practice, although the assumption of block-like motion is violated, ≈1% measurement accuracy can be obtained, because fault slip (5 mm) is typically much smaller than the width of the fault zone (e.g., 5 m; Bilham and Castillo, 2020).

Creepmeters often underestimate fault-zone slip because the fault is frequently associated with a shear zone that extends beyond the aperture sensed by the instrument, the deformation zone of the fault is wider than the instrument rig (Bilham and Castillo, 2020). Although the mechanical arrangement described earlier results in a large dynamic range, it comes with a measurement penalty because of frictional components in the sensor that result in stiction. Stiction is a stick-slip instrumental artifact caused by friction between the rod and its conduit, and from the bearings in the Hall sensor and tensioning pulleys. In a newly installed instrument, these effects are observed to be less than 10 μm, and when present occur with time durations of less than 1 s. Offsets occur in the data at the time of downloading due to manual disturbances to the instrument; however, a truck may be driven over the buried instrument without inducing stiction jumps (Bilham and Castillo, 2020).

Creepmeters on the western Dinaric Faults

Hall-effect creepmeters have been installed in major active seismogenic faults of the world: San Andreas Fault (USA), Eastern and North Anatolian Fault, Chaman Fault (Pakistan), Dead Sea Fault (Israel). All are faults with strong, frequent seismicity and fast deformation rates.

In contrast to western Dinarides, ie. western Dinaric Faults, exhibit moderate instrumental and strong historical seismicity and slow deformation rates of 2-4 mm/year (Serpelloni et al., 2018, Vičič et al., 2019). In order to identify potential shallow creep a project of installing creepmeters on them started in summer 2022. At the moment there are 3 instruments installed.

Two instruments on the Idrija Fault (Fig. 1), and one on the Raša Fault. The micro locations of the instruments were chosen on the basis of paleoseismic trenching and geologic field investigations along with remote sensing techniques. The telemetry-enabled instruments, logging data at 1-minute intervals and transmitting updates every hour, hold the promise of capturing even the subtlest indications of fault creeping activity.

The instrument on the Raša Fault is installed on a fault scarp, identified as a surface rupture via paleoseismological trenching (Aoudia, 2023: unpublished work of ICTP) in colluvial sediments. First instrument on the Idrija Fault was installed in alluvial sediments, identified surface rupture via paleoseismological trenching; Grützner et al., 2021), the second one is installed on a colluvial wedge.

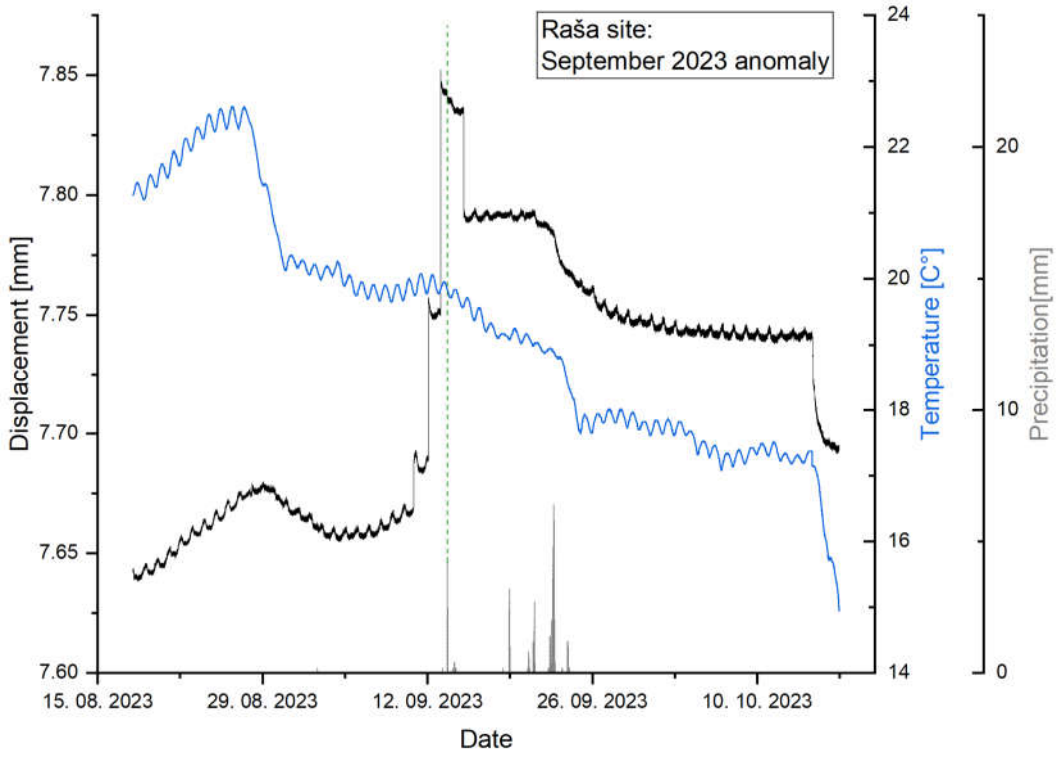

Figure 3: Anomalous displacements in September of 2023. Green dashed line marks the peak precipitation after the anomalous displacement.

The deployment of Hall-effect creepmeters on the western Dinaric Faults marks a crucial step in understanding the seismic behavior and deformation patterns of this region. Although no definitive evidence of creeping behavior has been observed thus far due to the absence of

major seismic events, anomalous displacements unrelated to heavy rainfall or temperature effects suggest the importance of continuous monitoring. As the project progresses, these Hall-effect creepmeters provide invaluable insights into the dynamic geological processes shaping the western Dinarides, contributing to enhanced seismic hazard assessments and the development of more effective risk mitigation strategies in this seismically active region.

The study is carried out within the framework of the Karst Research Programme (P6-0119) and Infrastructure Programme (I0-E017), all financially supported by the Slovenian Research and Innovation Agency and the project operation "Development of research infrastructure for the international competitiveness of the Slovenian RRI space - RI-SI-EPOS" and EC Horizon 2020 project EPOS SP.

Literature

Aoudia. A. (2023). Surface ruptures on the Raša Fault; unpublished work of ICTP.

Bilham, R., Ayruk, T. E., Turğut, M., İrgüren, R., Köküm, M., Elhisso, A., Farımaz, İ., Doğan, U. (2023). Afterslip and triggered slip following the 6 Feb 2023 Kahramanmaras earthquakes, East Anatolian Fault, Turkiye. Conference Proceedings of MedGU 2023, Istanbul.

Bilham, R., Castillo, B. (2020). The July 2019 Ridgecrest, California, Earthquake Sequence Recorded by Creepmeters: Negligible Epicentral Afterslip and Prolonged Triggered Slip at Teleseismic Distances. Seismological Research Letters; 91 (2A): 707–720. doi: https://doi.org/10.1785/0220190293.

Blanpied, M. L., Lockner, D. A, Byerlee, J. D. (1991), Fault stability inferred from granite sliding experiments at hydrothermal conditions, Geophys. Res. Lett., 18(4), 609–612, doi:10.1029/91GL00469.

Serpelloni, E., Pintori, F., Gualandi, A., Scoccimarro, E., Cavaliere, A., Anderlini, L., et al. (2018). Hydrologically induced karst deformation: Insights from GPS measurements in the Adria-Eurasia plate boundary zone. Journal of Geophysical Research: Solid Earth, 123, 4413– 4430. https://doi.org/10.1002/2017JB015252.

Grützner, C., Aschenbrenner, S., Jamšek Rupnik, P., Reicherter, K., Saifelislam, N., Vičič, B., Vrabec, M., Welte, J., and Ustaszewski, K. (2021). Holocene surface-rupturing earthquakes on the Dinaric Fault System, western Slovenia, Solid Earth, 12, 2211–2234, https://doi.org/10.5194/se-12-2211-2021.

Jolivet, R., Lasserre, C., Doin, M. P., Peltzer, G., Avouac, J. P., Sun, J., Dailu, R. (2013). Spatio-temporal evolution of aseismic slip along the Haiyuan Fault, China: Implications for fault frictional properties, Earth Planet. Sci. Lett., 377–378, 23–33, doi: 10.1016/j.epsl.2013.07.020.

Kaneko, Y., Fialko, Y., Sandwell, D. T., Tong, X., Furuya, M. (2013). Interseismic deformation and creep along the central section of the North Anatolian Fault (Turkey): InSAR observations and implications for rate-and-state friction properties, J. Geophys. Res. Solid Earth, 118, 316–331, doi:10.1029/2012JB009661.

Lindsey, E. O., Fialko, Y., Bock, Y., Sandwell, D. T., and Bilham, R. (2014). Localized and distributed creep along the southern San Andreas Fault, J. Geophys. Res. Solid Earth, 119, 7909–7922, doi:10.1002/2014JB011275.

Tong, X., Sandwell, D. T., Smith-Konter, B. (2013). High-resolution interseismic velocity data along the San Andreas Fault from GPS and InSAR, J. Geophys. Res. Solid Earth, 118, 369–389, doi:10.1029/2012JB009442.

Vičič, B., Aoudia, A., Javed, F., Foroutan, M., Costa, G. (2019). Geometry and mechanics of the active fault system in western Slovenia 2019. Geophysical Journal International, Volume 217, 3, 1755–1766. https://doi.org/10.1093/gji/ggz118.